Biomechanics of Extreme Lateral Lumbar Fusion with Different Internal Fixation Methods：A Finite Element analysis

Xiao-hua Li
The Third Hospital of Hebei Medical University
Li-jun She
Fifth Hospital of Shijiazhuang
Wei Zhang (sjzsdyyy@yeah.net)
The Third Hospital of Hebei Medical University
Xiao-dong Cheng
The Third Hospital of Hebei Medical University
Jin-peng Fan
First Hospital of Shijiazhuang

Research Article

Keywords: extreme lateral lumbar fusion, finite element analysis, internal fixation, adjacent segment degeneration, cage subsidence

Posted Date: September 22nd, 2021

DOI: https://doi.org/10.21203/rs.3.rs-907659/v1

Abstract

Background: Establishing a normal L3-5 model and using finite element analysis to explore the biomechanical characteristics of extreme lateral lumbar fusion (XLIF) with different internal fixation methods.

Method: The L3-5 CT image data of a healthy adult male volunteer were selected to establish a normal lumbar finite element model (M0). The range of motion (ROM) of L3-4 and L4-5, under flexion, extension, left bending, right bending, left rotation, and right rotation, together with L3-4 disc pressure was analyzed. Then the L4-5 intervertebral disc was excised and implanted with a cage, supplemented by different types of internal fixation, including lateral two-hole plate model (M1), lateral four-hole plate model (M2), VerteBRIDGE plating model (M3), lateral pedicle model (M4), posterior unilateral pedicle screw model (M5)and posterior bilateral pedicle screw model (M6) . The ROM ,the maximum stress value of the cage , and the maximum stress value of the intervertebral disc of L3-4 were analyzed and studied .

Results: The ROM of L3-4 and L4-L5 segments in the validation model under various motion states was basically consistent with previous reports. The lumbar finite element model was validated effectively. After XLIF-assisted internal fixation, the range of activity in L3-4 segments of each internal fixation model was greater than that of the normal model under various working conditions, among which the M5、M6 model had the larger range of activity in flexion and extension. After the internal fixation of L4-5 segments, the mobility in M1-M6 was significantly reduced under various motion patterns. In terms of flexion and extension, the posterior pedicle fixation model (M5、M6) showed a significant reduction,followed by M2. The maximal von mises cage stress of M1 was obviously greater than that of other models (except the left bending). Compared with M0, the intervertebral disc stress of M1-M6 at L3-4 segments was increased.

Conclusions: It is recommended that the posterior bilateral pedicle screw model is the first choice, followed by the lateral four-hole steel plate model for fixation during XLIF surgery. However, it is still necessary to be aware of the occurrence of adjacent segment degeneration (ASD) in the later stage.

Introduction

Interbody fusion is a classic surgical method for treating degenerative diseases of the lumbar spine. Traditional lumbar interbody fusion involves heavy pulling of soft tissue dissection, dural sac and nerve root, resulting in more postoperative complications. Extreme lateral interbody fusion (XLIF), proposed by Ozgur et al. [1] in 2006, was a surgical method that can be used to gain access to the lumbar spine via a lateral approach that passes through the retroperitoneal fat and psoas major muscle. The advantages of XLIF include no pulling of peripheral tissues such as nerves, blood vessels and peritoneum, and no need to enter the spinal canal for operation, reducing the possibility of injury to the dural sac and cauda equina, effectively avoiding the risks caused by anterior and posterior surgeries, with fewer complications, and extensive clinical application [2–7]. At present, there are few reports on the biomechanics of XLIF

internal fixation. Conventional biomechanics tests, such as animal experiments and cadaver specimens tests, cannot fully reflect the real biomechanical changes of the lumbar spine. Moreover, due to the particularity of the human body, the experimental cost is high, and the reproducibility is low. However, the three-dimensional finite element analysis is highly repeatable and can simulate the complex mechanical environment of the human lumbar spine in digital form. It is more vivid, practical and scientific, and is widely used in the field of spine biomechanics. This study aims to use finite element analysis to compare the biomechanical characteristics of XLIF with various internal fixations, and provide a theoretical basis for choosing the best internal fixation scheme.

Materials And Methods

Design

Three-dimensional finite element analysis test

Time and place

From March 2020 to June 2021, it was completed at the Institute of Orthopedic Biomechanics, the Third Hospital of Hebei Medical University.

Research object

A healthy adult male volunteer, who is 30 years old, 178cm tall, and 72kg, was selected. He had no history of low back pain and lower extremity pain, and his physical examination was normal. There were no obvious spinal lesions, deformities, tumors, injuries, and other manifestations on routine X-ray and CT examinations.

CT data acquisition

A 64-slice spiral CT from Siemens of Germany was used to continuously scan the L3-5 segment with a thickness of 1.0mm, and the tomographic image was obtained and saved in the standard DICOM format.

Construction of the normal model

The saved CT image file in DICOM format was imported into Mimics 14.01 software. First, bone tissue was processed by threshold segmentation, and surrounding tissue structure and editing mask were removed in parallel. Then 3D reconstruction was carried out to preliminarily build the L3-5 3D model, which was stored in STL format. The STL format model is imported into Geomagic 2013 software (Geomagic, Research Triangle Park NC, USA) and saved as an STP solid model through deburring and

smooth processing. After that, the solid model is imported into NX 12.0 software (Siemens Product Lifecycle Management Software Inc., USA), and 3D models of intervertebral disc and articular cartilage were established by stretching and Boolean operation commands. Finally, the models obtained in NX were successively imported into Hypermesh14.0 (Altair Company, USA) software in STP format to divide the grid; C3D10M mesh type was used in the vertebral body, and C3D20 mesh type was used in the nucleus pulposus.

Seven kinds of ligament models: anterior longitudinal ligament (ALL), posterior longitudinal ligament (PLL), ligamentum flavum (LF), interspinous ligament (ISL), supraspinous ligament (SSL), intertransverse ligament (ITL), and capsular ligament (CL), were constructed, according to the actual structure of the human anatomy atlas [8]. The ligament models were established by truss unit. The surface-to-surface contact element was used to simulate the articular surface. The friction coefficient between the articular surfaces was set to 0.1, and the strength of the joint capsule ligament was to 200N/mm. Both the bony structure and the intervertebral disc were assumed to be isotropic elastic materials, which were described by the two parameters of elastic modulus and Poisson's ratio. Ligament was a material that can only withstand tensile loads and had a zero response under compression. The material properties were quoted from literature [9-12], as shown in Table 1.

Table 1
Properties of material in the lumbar spine finite element models

Component	Young's modulus（MPa）	Poisson's ratio
Cortical bone	12000	0.3
Cancellous bone	100	0.2
Posterior element	3500	0.25
Endplate	1000	0.4
Annulus	4.2	0.45
Nucleus pulposus	1.0	0.4999
Articular cartilage	10	0.4
ALL	7.8	0.3
PLL	10	0.3
LF	15	0.3
ISL	10	0.3
SSL	8	0.3
ITL	10	0.3
CL	7.5	0.3

Validation of normal lumbar spine finite element

First, the weight of the upper body of the human body was simulated; the lower edge of the L5 vertebral body was fixed; and a 7.5 N-m [13] moment with a compressive preload of 500 N was imposed on the superior surfaces of the L3 vertebral body. Then, we calculated the range of motion (ROM) of the L3-4, L4-5 in flexion, extension, left bending, right bending, left rotation, and right rotation. The results showed that the ROM of the L3-4 and L4-5 segments in the model was basically consistent with that reported by Shim, et al. and Jiang, et al.[14-15], and it was all within a standard deviation range (Table 2) . This proves that the model is valid and can be used for further experimental research.

Table 2
Comparison of M0 with Jiang and Shim, etc.

Motion state（°）	L3-4			L4-5		
	M0	Jiang W et al	Shim, et al.	M0	Jiang W, et al	Shim, et al
Flexion	3.64	3.9	4.36±0.78	5.54	6.6	5.48±0.88
Extension	2.82	2.8	2.97±0.37	2.95	4.4	2.79±0.42
Left bending	1.99	1.80	1.76±0.72	2.91	2.80	2.23±1.01
Right bending	1.98	2.00	1.76±0.72	2.74	2.90	2.23±1.01
Left rotation	1.51	1.60	1.45±0.58	2.21	2.70	1.90±0.99
Right rotation	1.17	1.60	1.45±0.58	2.03	2.20	1.90±0.99

Establishment of XLIF finite element model

In NX 12.0 software (Siemens Product Lifecycle Management Software Inc., the United States), the screw rod internal fixation system model, the two-hole plate internal fixation model, the four-hole plate internal fixation model, VerteBRIDGE plating model and the intervertebral fusion cage model were drawn and established, and then optimized and meshed. After that, its position was adjusted by simulating the implantation direction of the steel plate and screw during the operation. Finally it was imported into Ansys to complete the establishment of the finite element model. The contact relationship between the intervertebral implant and the upper and lower endplates was set as surface-to-surface contact method to simulate the pre-fusion state, and the friction coefficient was set as 0.2 [16]. The Sextant system was simulated for pedicle screw fixation with a diameter of 6.5mm and a length of 50mm. The contact surface between the internal fixation system and the spine was set to be completely fixed, that is, looseness, displacement, breakage, etc. of the internal fixation were not considered. According to the research content, the models were named as M1 (lateral two-hole plate model), M2 (lateral four-hole plate model), M3 (VerteBRIDGE plating model), M4 (lateral pedicle model), M5 (posterior unilateral pedicle screw model), M6(posterior bilateral pedicle screw model) (see Figure 1). The lower edge of the L5 vertebral body was fixed to simulate the weight of the upper body of the human body, 500 N pressure was applied to the upper edge of the L3 vertebral body, and 7.5N.m torque was applied. The ROM of the above model was performed at L3-4 and L4-5 segments, including flexion, extension, left bending, right bending, left rotation, and right rotation. Data for maximum stress of intervertebral cage and maximum pressure of L3-4 intervertebral discs were collected and analyzed.

Results

ROM for the L3-4

Compared with M0, the ROM of the L3-4 segment of M1-M6 was increased under all motion patterns. Among them, the M5□M6 model had the larger range of activity in flexion and extension, the M6 models had the largest range of ROM in left bending and right bending, while the M1 and M2 models had the largest range of ROM in left and right rotation. As shown in Figure 2.

ROM for the L4-5

After internal fixation, the ROM of M1-M6 in the L4-5 segment was significantly reduced under all motion patterns. In terms of flexion and extension, the posterior pedicle fixation model (M5□M6) had a significant decrease ,followed by M2,while M1, M3, and M4 had relatively low decreases (see Figure 3).

Maximal von Mises stress of the Cage

As shown in Figure 4, the maximal von mises stress of the cage was obviously higher in M1 than that of other models (except for left bending). The stresses of M3 and M5 were also relatively high. In the left bending, the stress of M2, M1, and M4 were lower than other models.

Stress of the L3-4 Disc

As can be seen from Figure 5 (as follows). Compared with M0, the maximum stress of the L3-4 disc in M1-M6 was found to be higher under all loading conditions. In the flexion, M6 had the greatest stress . The stress of M1 was the highest in the extension. M1 and M2 had the greatest stress in left and right rotation.

Discussion

Finite element analysis is widely used in spinal biomechanics. At present, it is of great significance in the evaluation and analysis of spinal fusion and ASD[17–20]. In the past few years, XLIF was recognized and adopted by spinal surgeons worldwide. Although this operation has many advantages, the complications caused by it should not be ignored. Therefore, improving the stability of the fusion segment, reducing the incidence of cage subsidence and ASD is still the focus of future research.

After lumbar interbody fusion, the biomechanics of the entire spine will change. Its stress load transmission will also change accordingly. In order to stabilize the fusion segment, internal fixation is often supplemented. Clinical studies had shown that, although stand-alone cage can increase the stability of the segment, compared with the additional plate and pedicle screw fixation, the mobility of the fusion segment was significantly increased [21]. Through imaging analysis, Marchi et al. [22] found that the rate of cage subsidence of stand-alone during XLIF was as high as 30%. Thus, supplementary

fixation, such as pedicle screws, is recommended. Studies had shown that lumbar fixation and fusion can significantly reduce the ROM at the fusion level and provide strong stability[23]. Through research in this article, after internal fixation, the ROM of M1-M6 in the L4-5 segment was significantly reduced under all motion patterns. In terms of flexion and extension, the posterior pedicle fixation model (M5、M6) had a significant decrease, followed by M2, while M1, M3, and M4 had relatively low decreases. It showed that all fixation models could reduce the mobility of the fusion segment. The posterior pedicle fixation model provided high stability, followed by M2, while M1, M3, and M4 were relatively low.

Although much literature reported that there was no significant difference in stability and fusion rate between unilateral and bilateral pedicle fixation [24–25], many scholars still believed that the strength of unilateral fixation was not as stable as bilateral fixation [26–27]. Flexion and extension are the most frequent movements in daily human life. In this study, compared with other models, the pedicle screw fixation groups could significantly reduce the mobility of the fusion segment in terms of flexion and extension, indicating that the posterior pedicle fixation group can ensure the stability of the fusion segment, followed by the M2.

Cage subsidence is one of the common complications of lateral lumbar interbody fusion. Macki et al.[28] retrospectively analyzed 21 articles and included 1362 patients undergoing lateral lumbar interbody fusion, and identified that a subsidence incidence of 10.3% and a reoperation rate for subsidence of 2.7%. The maximum stress could be used to predict the sinking risk of the cage. The greater the stress, the higher the sinking risk [29–30]. Insufficient internal fixation strength was one of the important factors for cage subsidence. The use of supplemental internal fixation for lateral lumbar interbody fusion, such as bilateral pedicle screws, served to mitigate subsidence, protect the indirect decompression, and promote arthrodesis[31]. After fusion, the frictional contact between the cage and the endplate was likely to cause stress concentration. Compared with the unilateral fixation of pedicle screws, the bilateral pedicle screws can effectively control the stability of the index segment and reduce the load applied to the interbody fusion cage. In addition, bilateral fixation had relatively little stress damage to the fusion segment, and the protection of the cage itself was also relatively beneficial [32–33].

As shown in Fig. 4, the maximal von mises stress of the cage was obviously higher in M1 than that of other models (except for left bending), and the stresses of M3 and M5 were also relatively high.. In the left bending, the stress of M2, M1, and M4 were lower than in other models. This shows that M1 has a higher risk of cage subsidence, and the lateral internal fixation device can effectively share the stress of the cage during lateral bending.

After lumbar spine fixation and fusion, the mobility of the fixed segment decreases, causing the center of rotation to shift, thereby changing the motion of adjacent segments. Therefore, only by increasing the mobility of adjacent segments to compensate for the loss of mobility of the entire spine caused by the reduction of the mobility of the fixed segment.

In our study, after internal fixation, the ROM and disc stress of each model in the L3-4 segment in all motion cases were greater than that of the normal model, whereas the M5□M6 model had the larger range of activity in flexion and extension,, M6 had a high ROM in left and right bending, and M1 and M2 had the largest ROM in left and right rotation. By analyzing from the stress of the L3/4 disc, it could be concluded that the M6 disc had the highest stress in flexion; M1 had the highest stress in l extension; M1 and M2 had the highest stress in left and right rotation. Increased ROM and intervertebral disc stress in adjacent segments after spinal internal fixation were considered to be the main risk factors for ASD[34–35],and ASD was considered to be the result of spinal fusion [36]. With the increase in the stress of the intervertebral disc in the adjacent segment, the intervertebral disc deforms, resulting in an increase in the mobility of the adjacent segment. Therefore, the increase in the mobility of the adjacent segment may be caused by the increase in the intervertebral disc stress. Moreover, the flexion and extension activities were more closely related to the course of ASD [37].

Overall, all internal fixation models increase the mobility of adjacent segments and the stress of the intervertebral disc. Although the increase in mobility and intervertebral disc stress was not proportional to the strength of internal fixation, ASD should be considered when performing XLIF surgery. In clinical practice, the incidence of ASD can be reduced by reducing the ROM and intervertebral disc stress in adjacent segments.

Our study was based on finite element analysis and has several limitations. First of all, the division of elements and the determination of boundary conditions in the modeling process were all artificial settings, which need to be compared with cadaver specimens and in vivo experiments. Secondly, the adult healthy volunteer was selected, degenerative factors were not considered, and the muscles were not modeled. Therefore, the force of the human body could not be fully simulated. Furthermore, the biomechanical effects of internal fixation and surgery was simplified.

Conclusion

In conclusion, all fixation models could reduce the mobility of the fusion segment. The posterior pedicle fixation model provided high stability, followed by the lateral four-hole steel plate model. All fixation models could increase the ROM and intervertebral disc stress in adjacent segments and increase the incidence of ASD. The stress of the cage in lateral two-hole plate model was the largest, followed by VerteBRIDGE plating model and posterior unilateral pedicle screw model, and the risk of cage subsidence is higher in the later stage. Therefore, it is recommended that the posterior bilateral pedicle screw model is the first choice, followed by the lateral four-hole steel plate model for fixation during XLIF surgery. However, it is still necessary to be aware of the occurrence of adjacent segment degeneration in the later stage.

Abbreviations

XLIF: Extreme lateral interbody fusion; ROM: range of motion; ASD: adjacent segment degeneration; ALL: anterior longitudinal ligament; PLL: posterior longitudinal ligament; LF: ligamentum flavum; ISL: interspinous ligament ; SSL: supraspinous ligament ; ITL: intertransverse ligament ; CL: capsular ligament.

Declarations

Acknowledgements

Not applicable.

Authors’contributions

Li Xiao-hua: Conceptualization, Methodology, Writing- Original draft preparation,Writing- Reviewing

She Li-jun, Cheng Xiao-dong: Data curation,,Software,Validation

Fan Jin-peng: Visualization, Investigation, Supervision.

Zhang We: Conceptualization, Writing- Reviewing and Editing

Funding

Not applicable.

Ethics approval and consent to participate

Not applicable.

Availability of data and materials

The datasets used and/or analyzed during the current study are available from the corresponding author upon reasonable request.

Consent for publication

Not applicable.

Competing interests

The authors declare that they have no competing interests.

References

1. Ozgur BM,Aryan HE,Pimenta L,et al.Extreme Lateral Interbody Fusion (XLIF):A novel surgical technique for anterior lumbar interbody fusion [J]. Spine J,2006,6(4): 435–443.
2. Dakwar, E., Cardona, R. F., Smith, D. A.,et al. Early outcomes and safety of the minimally invasive, lateral retroperitoneal transpsoas approach for adult degenerative scoliosis [J]. Neurosurgical focus.2010;28(3):E8.
3. Oliveira L, Marchi, L, Coutinho, E, et al. A radiographic assessment of the ability of the extreme lateral interbody fusion procedure to indirectly decompress the neural elements. Spine (Phila Pa 1976). 2010;35(26 Suppl):S331-337.
4. Elowitz, E. H, Yanni, D. S., Chwajol, M., et al. Evaluation of indirect decompression of the lumbar spinal canal following minimally invasive lateral transpsoas interbody fusion: radiographic and outcome analysis [J]. Minimally invasive neurosurgery. 2011;54 (5/6): 201–206.
5. Meredith DS, Kepler CK, Huang RC, et al. Extreme Lateral Interbody Fusion (XLIF) in the Thoracic and Thoracolumbar Spine: Technical Report and Early Outcomes [J] .HSS J. 2013;9(1):25–31.
6. Winder MJ, Gambhir S. Comparison of ALIF vs. XLIF for L4/5 interbody fusion: pros, cons, and literature review [J] .J Spine Surg. 2016;2(1):2–8.
7. Paterakis KN, Brotis AG, Paschalis A, et al.Extreme lateral lumbar interbody fusion (XLIF) in the management of degenerative scoliosis: a retrospective case series [J] .J Spine Surg. 2018;4(3):610–615.
8. Plaats AVD, Veldhuizen AG, Verkerke GJ. Numerical Simulation of Asymmetrically Altered Growth as Initiation Mechanism of Scoliosis. Ann Biomed Eng. 2007;35(7):1206–1215.
9. Goel VK, Monroe BT, Gilbertson LG, et al. Interlaminar shear stresses and laminae separation in a disc. Finite element analysis of the L3-L4 motion segment subjected to axial compressive loads. Spine (Phila Pa 1976). 1995;20(6):689–698.
10. Polikeit A, Ferguson SJ, Nolte LP, et al. Factors influencing stresses in the lumbar spine after the insertion of intervertebral cages: finite element analysis. Eur Spine J. 2003;12(4):413–420.
11. Ding JY, Qian S, Wan L, et al. Design and finite-element evaluation ofa versatile assembled lumbar interbody fusion cage. Arch Orthop Trauma Surg. 2010;130(4):565–571.
12. Song C, Li XF, Liu ZD, et al. Biomechanical assessment of a novel L4/5 level interspinous implant using three dimensional finite element analysis. Eur Rev Med Pharmacol Sci. 2014;18(1):86–94.
13. Schmidt H,Heuer F,Claes L,et al.The relation between theinstantaneous center of rotation and facet joint forces-A finiteelement analysis.Clin Biomech (Bristol,Avon). 2008; 23(3): 270–278.
14. Shim CS, Park SW, Lee SH, et al. Biomechanical evaluation of an interspinous stabilizing device, Locker[J]. Spine (Phila Pa 1976). 2008, 33(22): 820–827.

15. Wei J, Wei L, Feng Y, et al. Stress changes of intervertebral disc after fusion of L4/5 facet joints: a finite element analysis[J]. Chin J Spine Spinal Cord. 2017;27(5):441–448.
16. Ambati D V, Wright E K Jr, Lehman R A Jr,et al. Bilateral pedicle screw fixation provides superior biomechanical stability in transforaminal lumbar interbody fusion: a finite element study [J].Spine J. 2015 ;15(8):1812–1822.
17. Srinivas GR, Deb A, Kumar MN.Long-Term Effects of Segmental Lumbar Spinal Fusion on Adjacent Healthy Discs: A Finite Element Study[J].Asian Spine J.2016;10(2):205–214.
18. Srinivas GR, Kumar MN, Deb A.Adjacent Disc Stress Following Floating Lumbar Spine Fusion: A Finite Element Study[J]. Asian Spine J.2017;11(4):538–547.
19. Cho PG, Ji GY, Park SH, et al. Biomechanical Analysis of Biodegradable Cervical Plates Developed for Anterior Cervical Discectomy and Fusion[J].Asian Spine J. 2018;12(6):1092–1099.
20. Wang BJ, Hua WB,Ke WC, et al. Biomechanical Evaluation of Transforaminal Lumbar Interbody Fusion and Oblique Lumbar Interbody Fusion on the Adjacent Segment: A Finite Element Analysis[J].World Neurosurg. 2019;126:e819-e824.
21. Shasti M, Koenig SJ, Nash AB, et al. Biomechanical evaluation of lumbar lateral interbody fusion for the treatment of adjacent segment disease[J]. Spine J, 2019,19(3):545–551.
22. Marchi L, Abdala N, Oliveira L, et al. Radiographic and clinical evaluation of cage subsidence after stand-alone lateral interbody fusion[J]. J Neurosurg Spine. 2013, 19(1):110–118.
23. Haddas R,Xu M, Lieberman I, et al. Finite Element Based-Analysis for Pre and Post Lumbar Fusion of Adult Degenerative Scoliosis Patients[J].Spine Deform. 2019;7(4):543–552.
24. Phan K, Leung V, Scherman DB, et al. Bilateral versus unilateral instrumentation in spinal surgery: Systematic review and trial sequential analysis of prospective studies[J]. J Clin Neurosci. 2016;30:15–23.
25. Chen DJ, Yao C,Song QW,et al. Unilateral versus Bilateral Pedicle Screw Fixation Combined with Transforaminal Lumbar Interbody Fusion for the Treatment of Low Lumbar Degenerative Disc Diseases: Analysis of Clinical and Radiographic Results[J].World Neurosurg. 2018; 115: e516-e522.
26. Duncan JW, Bailey. An analysis of fusion cage migration in unilateral and bilateral fixation with transforaminal lumbar interbody fusion[J]. Eur Spine J. 2013 ;22(2):439–445.
27. Pan FM, Wang SJ, Yong ZY, et al. Risk factors for cage retropulsion after lumbar interbody fusion surgery: Series of cases and literature review[J]. Int J Surg. 2016;30:56–62.
28. Macki M, Anand SK, Surapaneni A, et al. Subsidence Rates After Lateral Lumbar Interbody Fusion: A Systematic Review[J]. World Neurosurg. 2019;122:599–606.
29. Tsuang YH, Chiang YF, Hung CY, et al. Comparison of cage application modality in posterior lumbar interbody fusion with posterior instrumentation–a finite element study[J].Med Eng Phys. 2009;31(5):565–570.
30. Ouyang PG Lu T, He XJ, et al. Biomechanical Comparison of Integrated Fixation Cage Versus Anterior Cervical Plate and Cage in Anterior Cervical Corpectomy and Fusion (ACCF): A Finite Element

Analysis[J].Med Sci Monit. 2019, 25: 1489–1498.

31. Le TV, Baaj AA, Dakwar E, et al. Subsidence of polyetheretherketone intervertebral cages in minimally invasive lateral retroperitoneal transpsoas lumbar interbody fusion. [J].Spine (Phila Pa1976) .2012,37(14):1268–1273.
32. Cheng FU,ï¼·ang YZ,ï¼ªiang YG, et al. Three-Dimensional Finite Element Analysis of Transforaminal Lumbar Interbody Fusion[J]. JOURNAL OF SHANGHAI JIAO TONG UNIVERSITY. 2015;49(12):1876–1881
33. Li J,Wang HG,Shang J,et al.Finite element analysis of stress distribution before and after segment fusion in transforaminal lumbar interbody fusion model[J].J Third Mil Med Univ. 2015;37(14):1449–1454.
34. Xia XP, Chen HL, Cheng HB. Prevalence of adjacent segment degeneration after spine surgery: a systematic review and meta-analysis[J]. Spine. 2013;38(7):597–608.
35. Hashimoto K, Aizawa T, Kanno H,, et al. Adjacent segment degeneration after fusion spinal surgery-a systematic review[J]. Int Orthop. 2019;43(4):987–993.
36. Alentado VJ, Lubelski D, Healy AT, et al. Predisposing characteristics of adjacent segment disease after lumbar fusion. Spine.2016;41(14):1167–1172.
37. Jiang S, Li WS. Biomechanical study of proximal adjacent segment degeneration after posterior lumbar interbody fusion and fixation: a finite element analysis[J].J Orthop Surg Res.2019; 14(1): 135.

Figures

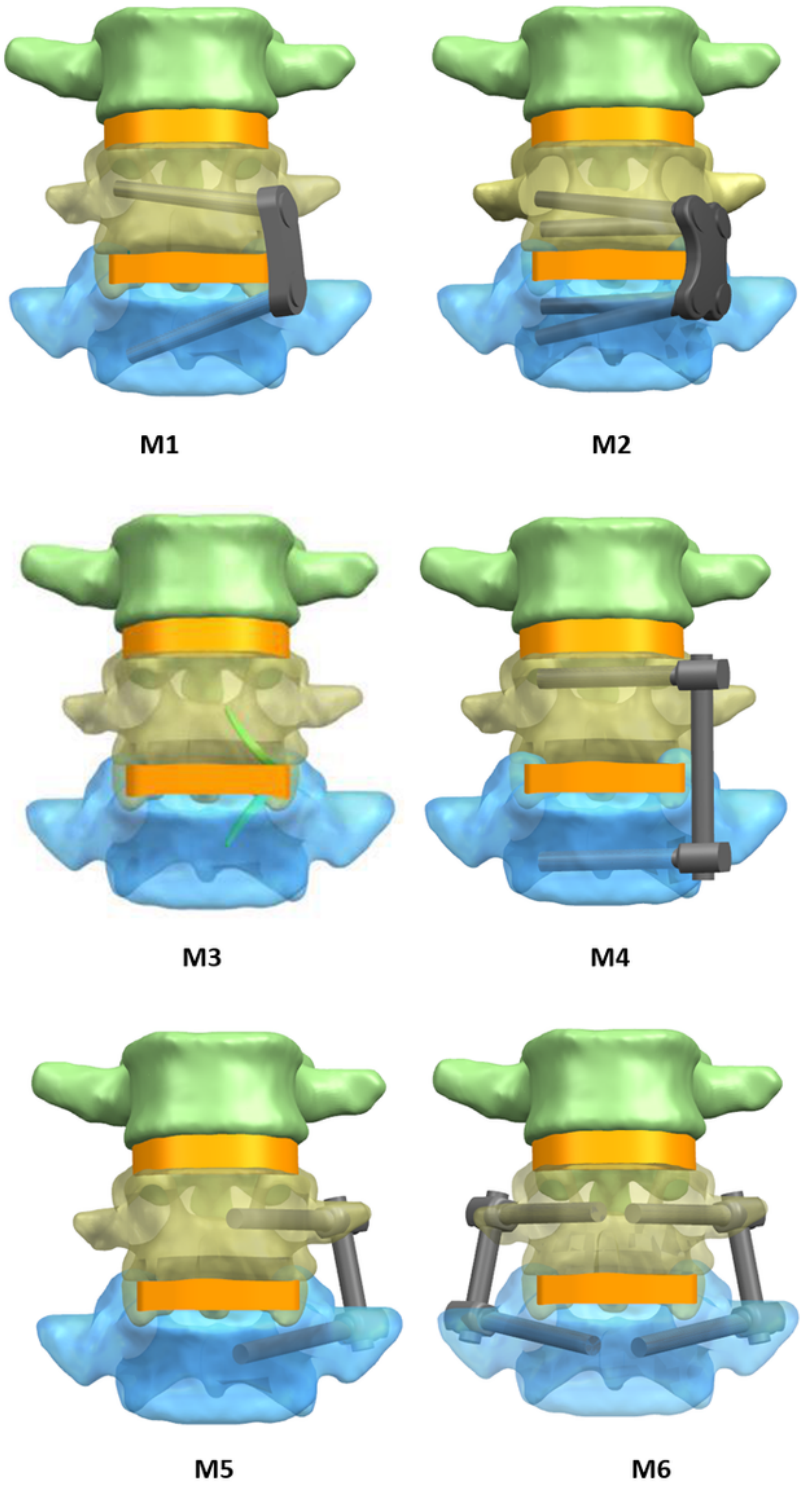

Figure 1

M1-M6 models :M1 (lateral two-hole plate model), M2 (lateral four-hole plate model), M3 (VerteBRIDGE plating model), M4 (lateral pedicle model), M5 (posterior unilateral pedicle screw model), M6(posterior bilateral pedicle screw model

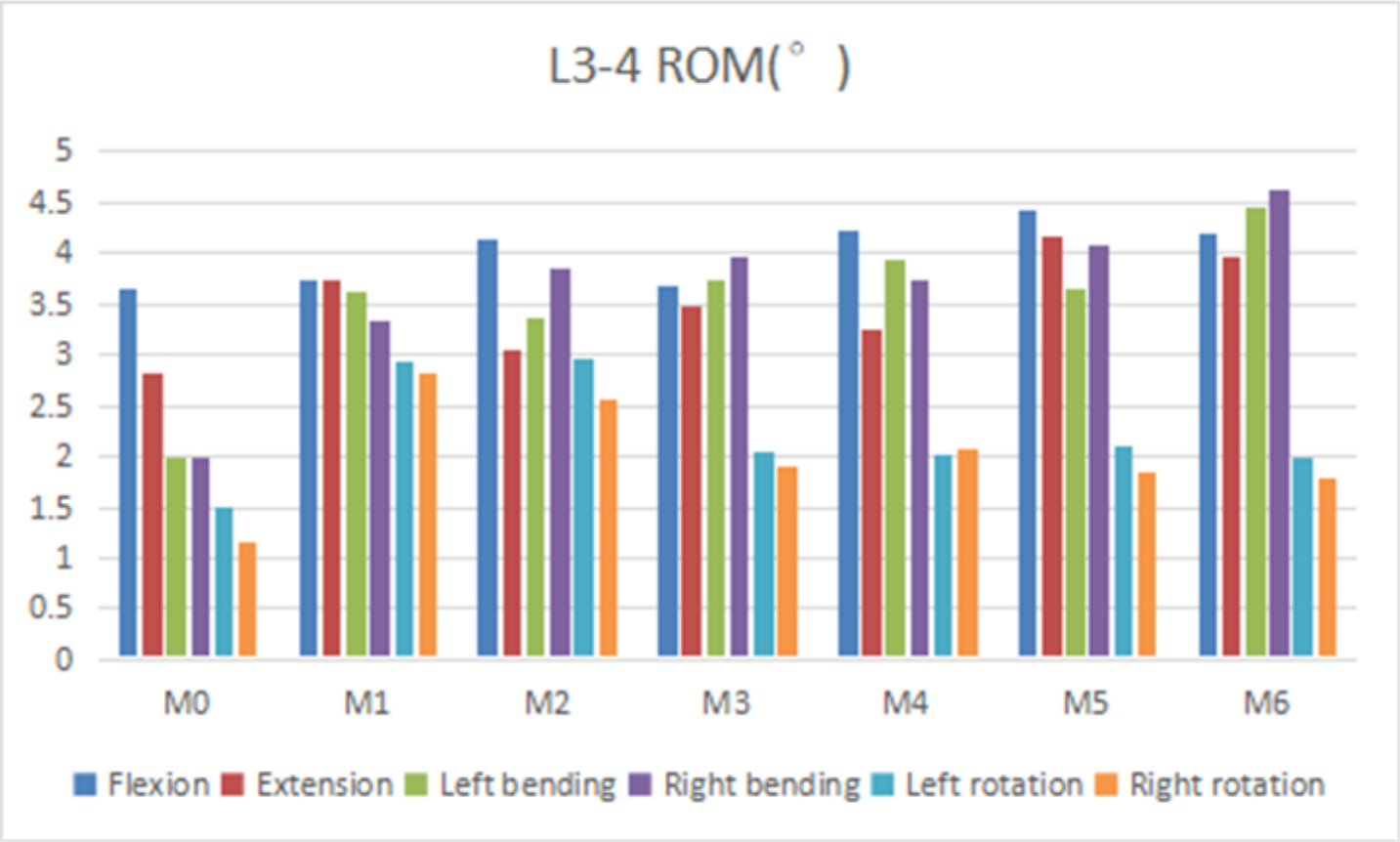

Figure 2

Comparison of the ROM for the L3-4 for seven types of models

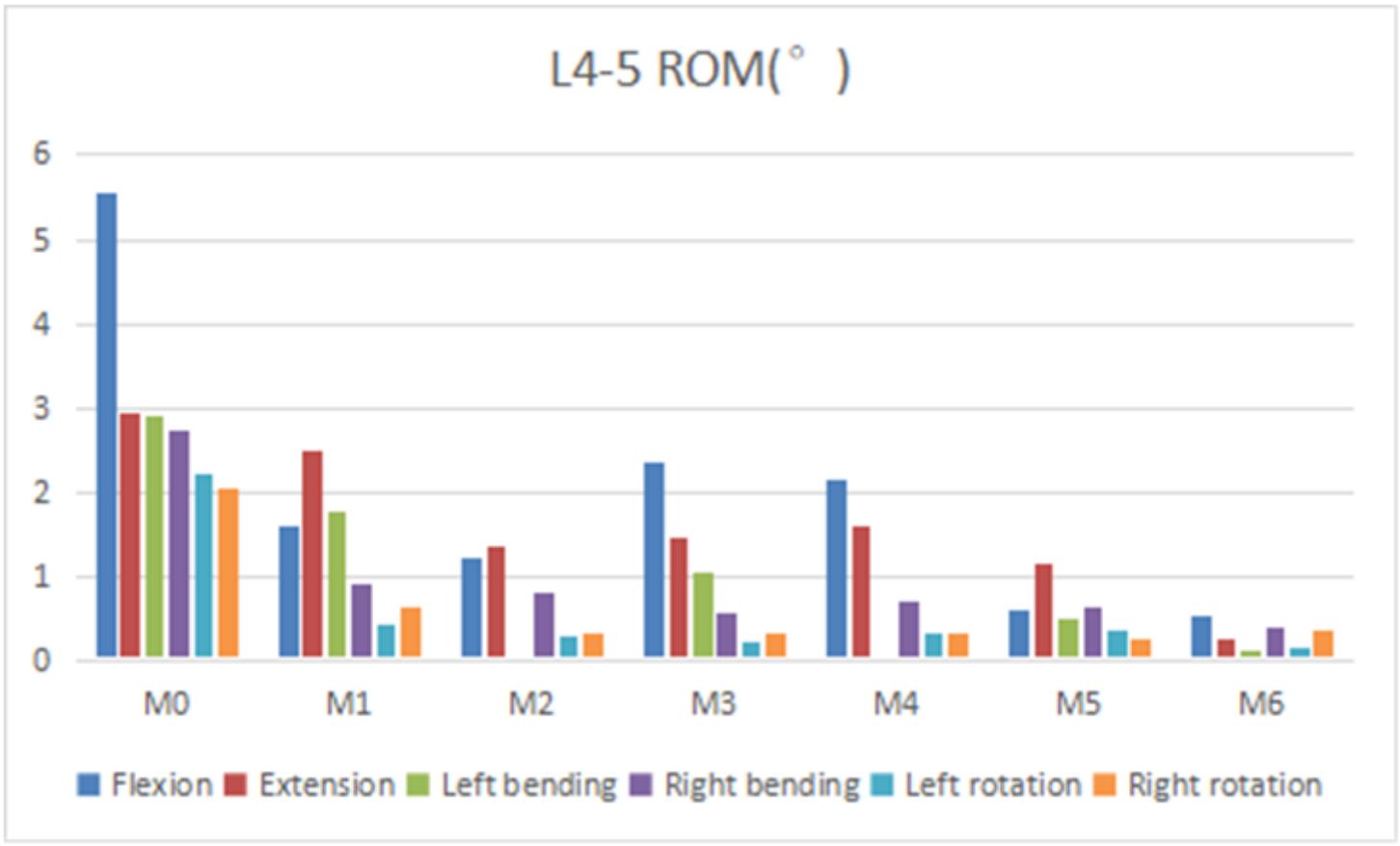

Figure 3

Comparison of the ROM for the L4-5 for seven types of models

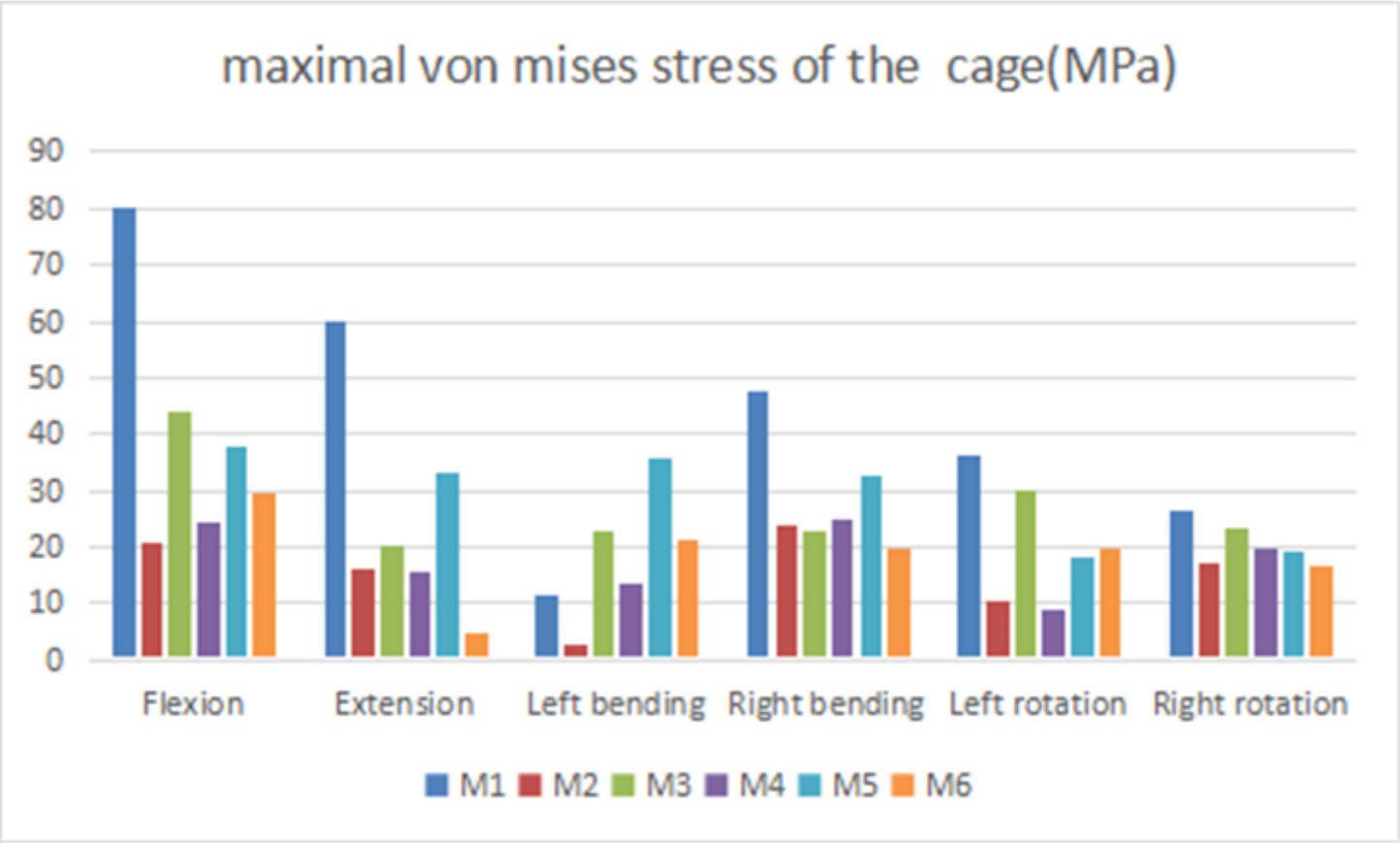

Figure 4

Comparison of the maximal von mises stress of the cage for six types of models

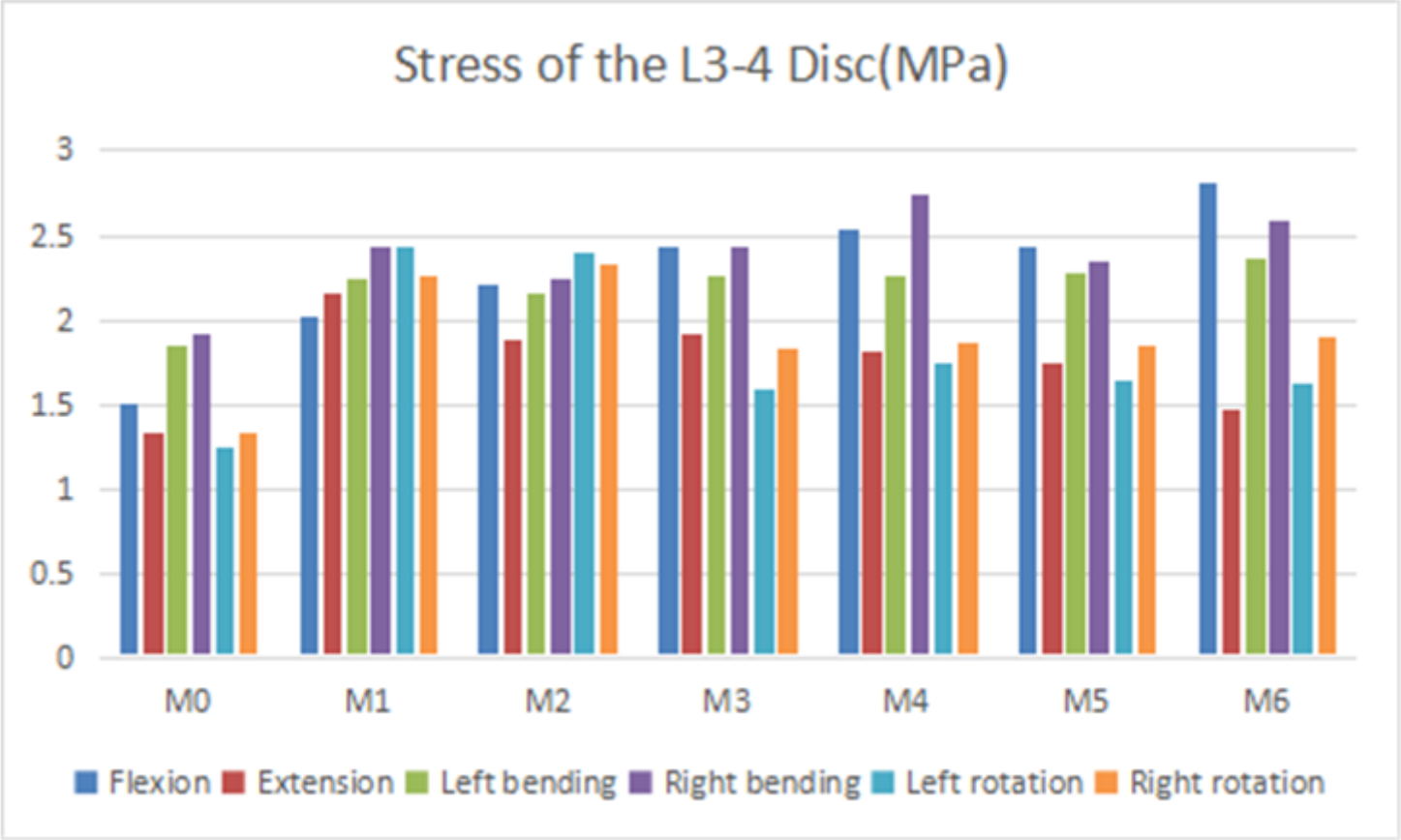

Figure 5

Comparison of the Stress of the L3-4 Disc for seven types of models